Hindawi Publishing Corporation
EURASIP Journal on Advances in Signal Processing
Volume 2007, Article ID 59704, 7 pages
doi:10.1155/2007/59704

Research Article

Efficient and Precise Processing for Squinted Spotlight SAR Through a Modified Stolt Mapping

Marijke Vandewal,[1] Rainer Speck,[2] and Helmut Süß[2]

[1] *Optronics and Microwave Department, Royal Military Academy, Renaissancelaan 30, Brussel 1000, Belgium*
[2] *Deutsches Zentrum für Luft-und Raumfahrt e.V. (DLR), Postfach 1116, Wessling 82230, Germany*

Received 26 January 2006; Revised 29 August 2006; Accepted 29 August 2006

Recommended by Christoph Mecklenbräuker

Processing of squinted SAR spotlight data is a challenge because of the significant range migration effects of the raw data over the coherent aperture time. Although in theory the (ω, k)-algorithm takes care of these aspects, its digital implementation requires a time-consuming interpolation step. Moreover, the limited precision of this interpolation can introduce distortions at the edges of the final image especially for squinted geometries. A wave number domain processing using a modified Stolt mapping will be developed and analyzed to enhance the quality of the final SAR image. Additionally, the proposed algorithm has a decreased computational load compared to the original (ω, k)-algorithm. Simulation results will validate the focusing and efficiency performances of the modified wave number domain algorithm.

1. INTRODUCTION

The atmospheric penetration and long-range capabilities of a synthetic aperture radar (SAR), combined with its high resolution, have made SAR imaging a favored approach for providing twenty-four hour all weather detection and recognition at "safe" standoff ranges. To achieve high resolution, a range dependent filter operation must be performed on the received raw data. The existing SAR processing algorithms differ in the approximations they use to combat problems as large data sets, range migration effects, secondary range decompression, and others. A majority of algorithms apply to raw data organized in an orthogonal (X, Y) grid (where X is the along-track and Y the across-track direction) and can be classified as stripmap mode processing algorithms, given the nature of stripmap data acquisition. Other algorithms work on a (range, azimuth angle) grid and can thus be classified as the pure spotlight mode processing algorithms, given the nature of spotlight data acquisition in a polar format. In order to process raw data acquired in a spotlight operating mode with a stripmap mode processing algorithm, these data have to be organized in an (X, Y) grid. As a result the range migration over the coherent aperture time as well as the change in range migration across the scene will be important, which makes processing of this kind of data challenging. These effects get even stronger when the squint angle increases, so in particular for a squinted spotlight operation mode, a high quality processor is mandatory.

The (ω, k)-algorithm [1–3] applies to raw data that are organized in an (X, Y) matrix and is thus by definition considered as a stripmap mode processing algorithm. This wave number domain processing is known for its elegant mathematical development since it deals with the SAR transfer function, without any approximation, through a change of variables (Stolt mapping) in the frequency domain. Although in theory the Stolt mapping takes care of the aspects typical for squinted spotlight SAR data, its digital implementation requires an interpolation step that can introduce distortions at the edges of the final image as the squint angle augments [4]. Increasing the precision of the interpolation kernel by using a longer interpolation function is possible; however, the computational efficiency of the algorithm will decrease significantly [5].

Solutions have been proposed in the literature to circumvent the disadvantages of the practical implementation of the (ω, k)-algorithm when processing squinted spotlight SAR data. In [4, 6] the most common version of the (ω, k)-algorithm is identified as a zero-Doppler processing, referring to the output geometry of the processed data which is based on the same orthogonal (X, Y) grid. In these papers

the degradations caused by the Stolt mapping on squinted data have been identified and quantified for a zero-Doppler output geometry. As a solution, a generalized wave number domain processing in an output geometry close to the acquisition geometry is proposed. This wave number "acquisition Doppler" processing allows a very efficient Stolt mapping and applies to all squint angles. In [7, 8] another solution for the (ω, k)-algorithm using the zero-Doppler output geometry has been proposed. Here the range walk (the linear component of the range migration) of the SAR raw data is removed before the actual processing. This leads to a limited skewing and shifting of the spectrum after the Stolt mapping, thus resulting in better performances regarding the overall resolution and the memory efficiency. On the other hand due to the removal of the range walk, the signal expression in the frequency domain has changed and the Stolt mapping requires a 2-dimensional interpolation. Knowing that the interpolation step is by far the most time consuming part of the code, the time efficiency of this processing can decrease.

The purpose of this paper is to improve the focusing performances of the (ω, k)-algorithm using the zero-Doppler output geometry for squinted spotlight data without increasing the computation time for a given set of parameters and for a given interpolation function length. As for the range-Doppler algorithm [1], where part of the Stolt mapping is replaced by an interpolation in the range-Doppler domain for moderate squint angles, this paper investigates such separation with respect to high squint angles to alleviate the interpolation step associated to the Stolt mapping. As an immediate consequence, for a given interpolation accuracy and thus efficiency of the algorithm, the focusing performances are improved, or, for a given focusing performance, the efficiency of the processor increases. The paper is organized as follows: first, a state of the art is given on the wave number domain zero-Doppler processing clarifying the causes of performance limitations for high squint angles. Next, a solution is proposed to circumvent these shortcomings through a modified Stolt mapping which will not decrease the time and memory efficiency. On the contrary, they both are enhanced as a consequence of the modified Stolt mapping. Finally, simulation results will validate the performances of the modified wave number domain processing. An unmanned aerial vehicle (UAV) from the high-altitude long-endurance (HALE) category has been chosen as the SAR platform. Indeed, the favored operating mode for reconnaissance missions of a SAR-UAV system is the squinted spotlight mode.

2. WAVE NUMBER DOMAIN PROCESSING

To understand the principle of the (ω, k)-algorithm, it is important to mathematically represent the raw SAR signal in the frequency domain after removal of the range chirp.

If $g(\tau)$ represents the pulse envelope, the received pulse, $h(\tau, t, R)$, is expressed by (1) after coherent demodulation for the removal of the carrier, and is the return of a point target on a zero reflecting background. The two-way antenna beam pattern is not represented since it does not contribute to the essence of the analyzed themes:

$$h(\tau, t, R) = g\left(\tau - \frac{2R}{c}\right) \cdot \exp\left\{-j\frac{4\pi}{\lambda}R\right\},$$
$$R = \sqrt{r_{\mathrm{sl}}^2 + V^2(t - t_0)^2}. \tag{1}$$

The variables and parameters in (1) are defined as follows:

(i) t and τ are slow time and fast time, respectively;
(ii) R is the slant range between a point scatterer and the antenna phase center and depends on slow time and the position of the point scatterer in the scene;
(iii) r_{sl} is the slant range at closest approach of a point scatterer and t_0 the time at which this closest approach takes place; the origin of the slow time axis is taken in the middle of the synthetic aperture interval;
(iv) V is the platform velocity;
(v) $g(\cdot)$ is the pulse envelope;
(vi) λ is the carrier wavelength of the transmitted signal;
(vii) c is the speed of light.

Fourier transforming this kernel to the range frequency domain (ν) results in (2), where $G(\nu)$ represents the envelope of the range frequency spectrum and ν_0 the carrier frequency of the transmitted signal:

$$H(\nu, t) = G(\nu) \cdot \exp\left\{-j\frac{4\pi}{c}R(\nu + \nu_0)\right\}. \tag{2}$$

For the Fourier transformation into the azimuth frequency domain (f), the stationary phase method can be applied [9]. The stationary point is reached for t^* for which the azimuth wave number, k_f, and the range wave number, k_ν, have been introduced in (3). The variable k_{ν_t} is considered as the total range wave number and k_{ν_0} as the range wave number related to the carrier frequency of the transmitted signal:

$$t^* = -\frac{r_{\mathrm{sl}}k_f}{V\sqrt{k_{\nu_t}^2 - k_f^2}} + t_0,$$
$$k_{\nu_t} = k_\nu + k_{\nu_0} = \frac{4\pi}{c}\nu + \frac{4\pi}{c}\nu_0, \tag{3}$$
$$k_f = \frac{2\pi}{V}f.$$

The azimuth Fourier transformation can now be approximated by (4), where unessential multiplicative constants are not represented:

$$H(k_{\nu_t}, k_f) \cong G(k_{\nu_t}) \cdot \exp\left\{-j\left(r_{\mathrm{sl}}\sqrt{k_{\nu_t}^2 - k_f^2} + k_f V t_0\right)\right\}. \tag{4}$$

Now the actual analysis of the wave number domain processing can begin. First, all the scatterers in the same range bin as the scene center will be correctly focused after multiplication with the phase reference function in (5), where r_{ref} refers to the slant range of the scene center at closest approach:

$$\phi_{\mathrm{ref}} = r_{\mathrm{ref}}\sqrt{k_{\nu_t}^2 - k_f^2}. \tag{5}$$

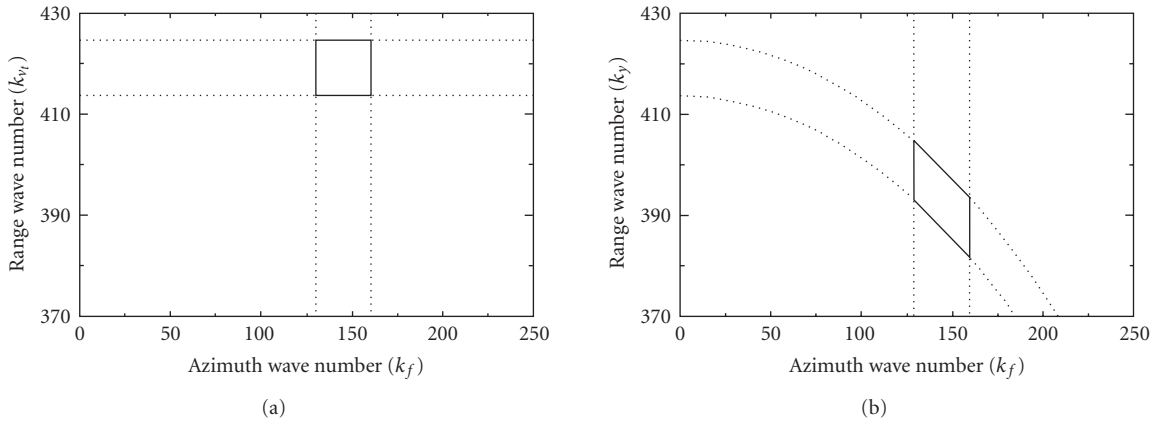

FIGURE 1: Illustration of the data spectrum before (a) and after (b) the Stolt mapping within the defined bandwidths (squint angle = 20°).

At this point all the point scatterers at the reference range r_{ref} are correctly focused and the defocusing of the other point scatterers increases with $(r_{\text{sl}} - r_{\text{ref}})$. Introducing an appropriate change of variables (6) will correctly focus the scatterers at all ranges and will lead to the signal in (7):

$$\begin{aligned} k_f &= k_f, \\ k_y &= \sqrt{k_{\nu_t}^2 - k_f^2}, \end{aligned} \tag{6}$$

$$S(k_y, k_f) = G(k_y) \cdot \exp\{-j((r_{\text{sl}} - r_{\text{ref}}) \cdot k_y + k_f V t_0)\}. \tag{7}$$

Figure 1 illustrates the range wave number before (a) and after (b) the Stolt mapping as a function of the azimuth wave number. The full line box on Figure 1(a) indicates the size of the data spectrum before the Stolt mapping: the two horizontal dotted lines delimit the range bandwidth and the two vertical dotted lines delimit the azimuth bandwidth for a 20° squint angle (using the parameters of Table 1 in Section 4). The change of variables of (6) transforms equidistant lines of constant total range wave number (the dotted horizontal lines on Figure 1(a)) into curves in k_y (the dotted curved lines on Figure 1(b)). This results in a skewing and a downward shifting of the data spectrum (as indicated by the full line box on Figure 1(b)).

A first immediate consequence is that the new samples are not equally sampled in k_y and thus interpolation is needed to allow inverse Fourier processing (to return to the time domain). A high quality interpolation kernel is required to avoid the introduction of artifacts at the edges of the final SAR image [4, 5] for high squint angles, where the skewing of the spectrum after the Stolt mapping becomes important. The nature of the interpolation function as well as its size are of importance, however, as mentioned before the increase of the latter will decrease significantly the computational efficiency of the processor.

A second consequence is that the computational efficiency of the (ω, k)-algorithm decreases with the squint angle. Indeed, looking at the full line box of Figures 1(a) and 1(b), an increase of the size of the data spectrum in the range wave number direction is noted. For the given set of parameters and a squint angle of 20°, the needed bandwidth in range after the Stolt mapping is more or less twice the range bandwidth of the data before the Stolt mapping.

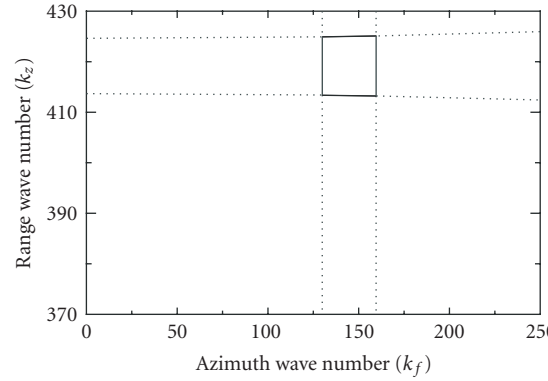

FIGURE 2: Illustration of the data spectrum after the modified Stolt mapping within the defined bandwidths (squint angle = 20°).

3. USE OF A MODIFIED STOLT MAPPING

The purpose of this paragraph is to propose a solution that will enhance the focusing performances of the wave number domain processor for a given interpolation kernel. Since the skewing of the spectrum has been identified in the previous section as the main cause of degradation effects at the edges of the image, the aim is to change the Stolt mapping of (6). A new change of variables is proposed in (8) to even out the skewing over the interval of the range wave numbers by taking the curvature of the carrier range wave number as the reference curve:

$$\begin{aligned} k_f &= k_f, \\ k_z &= \sqrt{k_{\nu_t}^2 - k_f^2} + \left(k_{\nu_0} - \sqrt{k_{\nu_0}^2 - k_f^2}\right). \end{aligned} \tag{8}$$

The impact of this change of variables is illustrated in Figure 2. The modified range wave number k_z is again represented

as a function of k_f. The full line box delimits the size of the data spectrum after the modified Stolt mapping. As intended, the skewing of the spectrum is reduced drastically and the simulation results in the next section show that the overall resolution performances are enhanced. A second consequence is that the size of the data spectrum did not change significantly, meaning that the computational efficiency of the modified (ω, k)-algorithm is now quasi-independent of the squint angle.

The resulting signal after the modified change of variables is given by (9). Comparing (9) with (7) shows that an unwanted phase term is present that needs to be corrected. Since this phase term only depends on range and on k_f, it can be eliminated by multiplying the data with the phase function of (10) in the range-Doppler domain. The extra computational load of this operation is negligible since it can be performed within the loop of the inverse Fourier transformation after the interpolation step:

$$H(k_z, k_f) \cong G(k_z) \cdot \exp\left\{ -j\left((r_{\text{sl}} - r_{\text{ref}}) \cdot \left(k_z - k_{\nu_0} + \sqrt{k_{\nu_0}^2 - k_f^2} \right) + k_f V t_0 \right) \right\}, \tag{9}$$

$$\phi_c = \exp\left\{ j(r_{\text{sl}} - r_{\text{ref}}) \cdot \left(-k_{\nu_0} + \sqrt{k_{\nu_0}^2 - k_f^2} \right) \right\}. \tag{10}$$

The physical interpretation of this modified change of variables can be easily done after expanding and rewriting the square root term as in [1] leading to (11):

$$\sqrt{k_{\nu_t}^2 - k_f^2} \cong \left(\underbrace{k_{\nu_0} D}_{\substack{\text{azimuth} \\ \text{modulation}}} + \underbrace{\frac{k_\nu}{D}}_{\substack{\text{range} \\ \text{migration}}} - \underbrace{\frac{k_f^2 k_\nu^2}{2k_{\nu_0}^3 D^3}}_{\text{SRC}} \right). \tag{11}$$

Higher-order terms have been neglected in (11) and D is denoted as the migration parameter, expressed by

$$D = \sqrt{1 - \frac{k_f^2}{k_{\nu_0}^2}}. \tag{12}$$

The three terms on the right-hand side of (11) represent, respectively, the azimuth modulation, the range migration (RM), and the secondary range compression (SRC). Indeed, the normal Stolt change of variables corrects for these three terms (and other higher-order terms that have been omitted in (11)) simultaneously through the Stolt mapping in the wave number domain. The azimuth modulation is the dominant term in (11) and is the main contributor to the shifting and the skewing of the spectrum after the Stolt mapping. When the same development as in (11) is done for the modified change of variables, it becomes clear that it is exactly that term which is cancelled out (13). The correction of the residual azimuth modulation is then done in the range-Doppler domain (see (10)):

$$\sqrt{k_{\nu_t}^2 - k_f^2} + \left(k_{\nu_0} - \sqrt{k_{\nu_0}^2 - k_f^2} \right) \cong \left(\underbrace{\cancel{k_{\nu_0} D}}_{\substack{\text{azimuth} \\ \text{modulation}}} + \underbrace{\frac{k_\nu}{D}}_{\substack{\text{range} \\ \text{migration}}} - \underbrace{\frac{k_f^2 k_\nu^2}{2k_{\nu_0}^3 D^3}}_{\text{SRC}} \right) + \left(k_{\nu_0} - \cancel{k_{\nu_0} D} \right). \tag{13}$$

Looking at the exact formulation of the range-Doppler algorithm [1], there is a strong analogy between this algorithm and the (ω, k)-algorithm using the modified Stolt mapping. Indeed, in both cases the azimuth modulation is corrected in the range-Doppler domain through a phase multiplication and the RM as well as the SRC are corrected through a mapping of the data. However, an important difference remains: in the range-Doppler algorithm, the mapping is done in the range-Doppler domain, whereas for the (ω, k)-algorithm this is performed in the wave number domain.

The main advantage is that through the modified Stolt change of variables the same efficiency is obtained as with the exact formulation of the range-Doppler algorithm but without making any approximations throughout the whole program.

Table 1: Simulation parameters.

Altitude	18 km
Velocity, V	175 m/s
Squint angle	20°
Pulse repetition frequency	500 Hz
Carrier frequency, ν_0	10 GHz
Chirp rate, γ	24.0 MHz/μs
Pulse length	10.9 μs
Aperture time	6.0 s
Range resolution	0.5 m
Azimuth resolution	0.5 m

4. SIMULATION RESULTS

The set of parameters in Table 1 has been used to simulate a raw data set for a squint angle of 20° (defined between the across-track direction and the antenna looking direction). The values of the platform related parameters correspond to the characteristics of a HALE UAV such as the Global Hawk. The squinted geometry has been defined in such a way that the slant range between the scene center and the antenna phase center in the middle of the aperture time is 40 km. The illuminated scene (600 m × 600 m) is composed of 9 point targets, distributed as in Figure 3 and the antenna points to a forward left direction as it travels in the positive direction of the azimuth axis below, applying the spotlight operation mode.

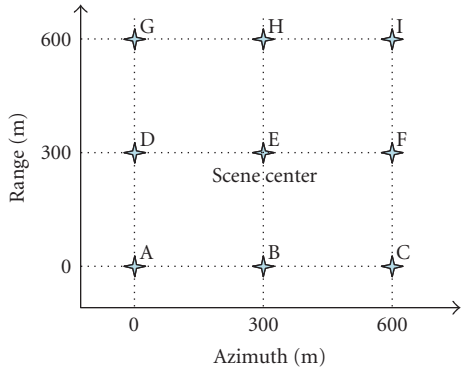

Figure 3: Geometry of the illuminated scene.

As mentioned in the previous sections, the focusing performances of the (ω, k)-algorithm using the zero-Doppler output geometry for squinted spotlight data can degrade at the edges of the image. This has been illustrated by analyzing the 3 dB-resolution in the azimuth and range direction of the processed point targets E (scene center), I and B. The cubic convolution has been used as the interpolation method since it closely approximates the theoretically optimum sinc interpolation function using cubic polynomials. The number of neighboring points used during the interpolation is limited to four (imposed by the used programming language) and an oversampling factor of 8 has been used to enhance the quality of the interpolation step. On Figure 4 the contours of magnitude of the processed point targets has been represented to give a qualitative impression of the difference in focusing performances across the illuminated scene. In the upper left corner these performances have been quantified by the exact value of the 3 dB-resolution in both directions (Az: azimuth, Ra: range).

These results show that the broadening of the azimuth resolution is rather high at the edges of the scene, especially at far range (broadening of 21% compared to the obtained azimuth resolution for the scene center).

Analogous to this analysis, the focusing performances of the modified (ω, k)-algorithm have been presented on Figure 5. For the far range point target the original azimuth broadening of 21% is diminished to 2%, thanks to the modified Stolt mapping. As an additional advantage, the time needed to process the data with the modified (ω, k)-algorithm is only 60% of the time that was required for the original wave number domain processing. As a result the computational efficiency of the modified wave number algorithm is similar to the one obtained when processing non-squinted raw data.

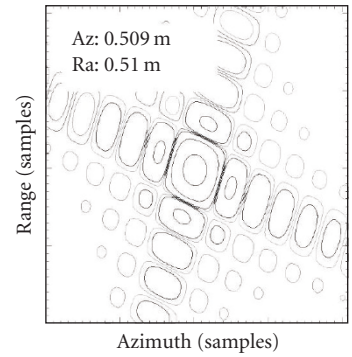

(a) Target E

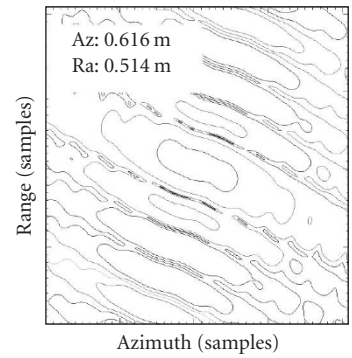

(b) Target I

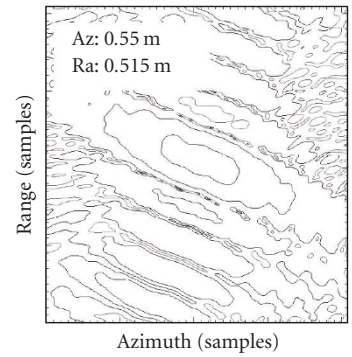

(c) Target B

Figure 4: Resolution analysis after processing with the original (ω, k)-algorithm (squint angle = 20°).

5. CONCLUSIONS

This paper described the state of the art of the (ω, k)-algorithm using the zero-Doppler output geometry when processing squinted spotlight data. The limitations of the digital implementation of this algorithm have been described as well as their impact on the overall focusing performances. A modified wave number domain algorithm has been proposed to improve these performances for a given set of parameters and a given interpolation kernel, typical for the (ω, k)-algorithm. As an additional advantage the computational efficiency of this new algorithm is expected to increase since the size of the data spectrum can be reduced to the size in case of no squint. The raw data of point targets at different ranges have been simulated and processed using a HALE UAV as the SAR platform. Simulations results have shown a significant improvement in the azimuth resolution when applying the modified wave number algorithm, especially at far

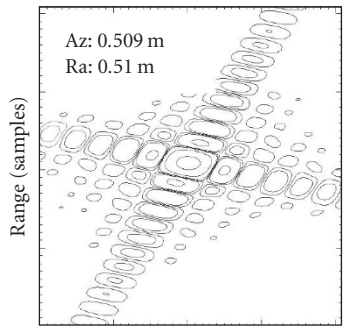

(a) Target *E*

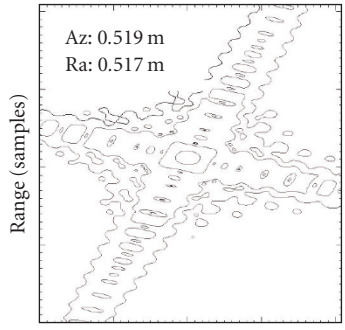

(b) Target *I*

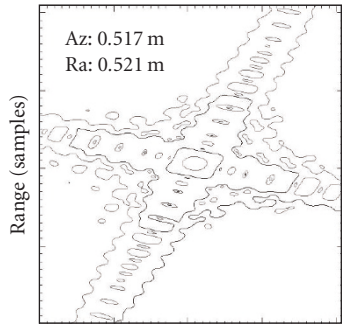

(c) Target *B*

Figure 5: Resolution analysis after processing with the modified (ω, k)-algorithm (squint angle = 20°).

range. Moreover, the overall computation time has been improved considerably by the proposed modifications and has been proven to be approximately independent of the value of the squint angle.

REFERENCES

[1] I. G. Cumming and F. H. Wong, *Digital Processing of Synthetic Aperture Radar Data*, chapter 5, 8, Artech House, Boston, Mass, USA, 2005.

[2] W. G. Carrara, R. S. Goodman, and R. M. Majewski, *Spotlight SAR Signal Processing Algorithms*, chapter 10, Artech House, Boston, Mass, USA, 1995.

[3] R. Bamler, "A comparison of range-Doppler and wavenumber domain SAR focusing algorithms," *IEEE Transactions on Geoscience and Remote Sensing*, vol. 30, no. 4, pp. 706–713, 1992.

[4] G. Fornaro, E. Sansosti, R. Lanari, and M. Tesauro, "Role of processing geometry in SAR raw data focusing," *IEEE Transactions on Aerospace and Electronic Systems*, vol. 38, no. 2, pp. 441–454, 2002.

[5] P. T. Gough and D. W. Hawkins, "Unified framework for modern synthetic aperture imaging algorithms," *International Journal of Imaging Systems and Technology*, vol. 8, no. 4, pp. 343–358, 1997.

[6] G. Fornaro, G. Franceschetti, and S. Perna, "Motion compensation of squinted airborne SAR raw data: role of processing geometry," in *Proceedings of IEEE International Geoscience and Remote Sensing Symposium (IGARSS '04)*, vol. 2, pp. 1518–1521, Anchorage, Alaska, USA, September 2004.

[7] P. Berens, "Extended range migration algorithm for squinted spotlight SAR," in *Proceedings of IEEE International Geoscience and Remote Sensing Symposium (IGARSS '03)*, vol. 6, pp. 4053–4055, Toulouse, France, July 2003.

[8] P. Berens, "Efficient wave number domain processing for squinted spotlight SAR," in *Proceedings of 5th European Conference on Synthetic Aperture Radar (EUSAR '04)*, vol. 1, pp. 171–174, Ulm, Germany, May 2004.

[9] M. Soumekh, *SAR Signal Processing*, John Wiley & Sons, New York, NY, USA, 1999.

Marijke Vandewal was born in Sint-Truiden, Belgium, in 1973. She received a B.S. degree in electronic engineering in 1996 from the Polytechnics Faculty of the Belgian Royal Military Academy (RMA). From 1996 to 2001 she served the Belgian Air Force working in the radar domain. In 2001, she started with a research project on SAR simulation, conducted under a joint supervision between the German Aerospace Center (DLR) and the RMA. In 2006, she obtained the Ph.D. degree in applied sciences at the Vrije Universiteit Brussel (VUB) in Belgium. Since her return to the RMA in 2001, she has been working as an Assistant in the Optronics, Microwave, and Radar Department. Her main research interests are in synthetic aperture radar (SAR), electromagnetic propulsion, laser applications, and imaging methods using electromagnetic waves in general.

Rainer Speck was born in Pforzheim, Germany, in 1962. He received the Dipl.-Ing. (M.S.E.E.) and the Dr.-Ing. (Ph.D.E.E.) degrees in electrical engineering from the University of Karlsruhe, Karlsruhe, Germany, in 1990 and 1994, respectively. Since 1996, he has been with the Department for Reconnaissance and Security of the Microwaves and Radar Institute, German Aerospace Center (DLR), Oberpfaffenhofen, Germany. Since 2000, he has been leading the SAR Simulation Research Group. His main research interests are in synthetic aperture radar (SAR), electromagnetic propagation, and scattering theory, with the focus on the development of end-to-end simulation tools for high-resolution SAR systems for air- and spaceborne reconnaissance.

Helmut Süß made his Diploma in physics in 1978 at the University of Mainz. In 1982, he obtained a Ph.D. degree at the University of Bochum. From April 1987 to March 1988 he obtained a Postdoctoral Fellowship from the US National Science Foundation at the JPL (California Institute of Technology); research topics: analysis of multisensor data, design of high-resolution aperture synthesis radiometer. In 1994, he was appointed as the Head of the Multisensor-Systems Group, and in 1996 as the Head of the Department for Reconnaissance Methods. Since 2001, he is Head of the Department for Reconnaissance and Security Responsibility for military activities and relations to the GE MoD, NATO, and WEU. In June 2006, he became Honorary Professor at the University of the German Armed Forces for Radar and Laser Methods. His research areas are design and analysis of high-resolution SAR systems for air- and spaceborne reconnaissance, design and analysis of aperture synthesis radiometer systems, detection of antipersonnel mines, spatial resolution improvement of microwave imaging systems, microwave signature modeling and analysis, and image processing for polarimetric classification and automatic target recognition.